



Methods to Improve the Spatial Resolution of EEG

Ramesh Srinivasan

The Neurosciences Institute, 10640 John Jay Hopkins Drive, San Diego, USA

Abstract. Theoretical models and experimental EEG data were examined to quantify the spatial resolution of scalp surface recordings of EEG. The results suggest that scalp EEG electrodes are mostly sensitive to activity correlated over large areas of the superficial neocortical surface, with smaller contributions from deeper sources. The surface Laplacian of the scalp surface potential is shown to be an estimate of the cortical surface potential. To accurately compute the surface Laplacian, the 3-dimensional spline algorithm has been developed to minimize aliasing errors by applying a smoothing filter based on the effective size of each electrode. The spline-generated surface Laplacian improves the spatial resolution of EEG by reducing the sensitivity of each electrode to only a local region of neocortical tissue beneath the electrode.

1. Introduction

EEG electrodes are separated from current sources in the brain by cerebrospinal fluid (CSF), the skull, and the scalp (Nunez, 1981). As a consequence, EEG has poor spatial resolution, which is qualitatively appreciated by many clinicians and researchers that use EEG. Unfortunately, this fact has been used to support the idea that a few (and often only one) point sources in the brain generate spontaneous EEG phenomena (e.g., alpha rhythm) or evoked potentials, since each source generates a potential distribution that is widespread over the scalp. In practice, many spatial patterns of EEG and evoked potentials can be reasonably fit (in a least-squares sense) by a few equivalent dipoles, or even just one. However, each equivalent dipole may only reflect the "center of mass" of a pattern of activity distributed throughout a region of the brain. The interpretation of dipole fits must be tempered by the consideration that there are many other possible solutions each of which is equally plausible, and that there may only be a few cases where the a priori assumption of a few point sources is justified. There is little evidence from intracranial recordings to support the contention that only a few sites in the brain are active in generating either evoked potentials or spontaneous EEG (Towle et al., 1998). Rather, there are likely to be spatio-temporal patterns of neural activity correlated at multiple spatial scales and distributed throughout the brain (Nunez, 1995).

Thus, there has been considerable motivation to approach the problem of EEG localization by developing methods to improve the spatial resolution of EEG without making assumptions about the quantity or distribution of sources in the brain. Two distinct methods

collectively termed high resolution EEG (Nunez et al., 1994) are being developed to estimate cortical surface potentials: cortical imaging (Sidman et al., 1991) and surface Laplacians (Law et al., 1993; Srinivasan et al., 1996; Babiloni et al., 1996). The cortical surface potential refers to the potential measured a smooth surface surrounding the volume of the brain, as in direct recordings from the human brain in surgical patients with surface grids (Towle et al., 1998), without accounting for the folds of the cortical surface. Cortical imaging refers to methods that estimate the cortical surface potential from the scalp potential (which is a well-posed problem) without making assumptions about the sources, but assuming an approximate volume conduction model of the head. The conductivity values of the tissue compartments of the head (white-matter, gray-matter, CSF, skull, and scalp) are not well-known, so that even an exact geometric model of the head is still only an approximate volume conduction model of the head. The surface Laplacian is the second spatial derivative of the scalp potentials, which is usually taken along an approximation to the surface of the head, such as the best-fit sphere. These two methods produce consistent estimates of cortical surface potentials, despite their distinct theoretical bases (Nunez et al., 1994). In this paper, we discuss the physical basis of surface Laplacian estimates, and make quantitative estimates of the spatial resolution of both potential and Laplacian EEG.

2. Spatial transfer function of the head

What is the relationship between the spatial distribution of activity within the brain and scalp potentials? The scalp potential due to a single current source in the brain is determined by the volume conduction of electric fields in a layered inhomogeneous medium (Nunez, 1981). Volume conduction is linear, so that the scalp potential due to multiple sources is simply the sum of the scalp potential due to each source. In this section, an approximate volume conduction model of the head will be used to make theoretical estimates of the transfer function between cortical current source distributions and scalp potentials.

2.1 Four concentric spheres model of the head

Four concentric spheres, which represent brain, CSF, skull, and scalp is a simple physical model of the volume conduction properties of the head. The details of this model can be obtained from the references (Srinivasan et al., 1996; Srinivasan et al., 1998a). The fundamental assumptions of the model are that Ohm's Law applies in each region and that capacitive effects are negligible. In this case, the scalp potential distribution depends on the magnitudes and locations of the current sources and the thickness and conductivity of the spherical shells (Nunez, 1981). In most of the simulations presented here, and unless otherwise noted, the head model parameters are assumed to be radii ($r_{\text{brain}}, r_{\text{CSF}}, r_{\text{skull}}, r_{\text{scalp}}$) = (8, 8.1, 8.7, 9.2) cm and conductivity ratios ($\sigma_{\text{brain/CSF}} = 0.2$, $\sigma_{\text{brain/skull}} = 80$, and $\sigma_{\text{brain/scalp}} = 1$). These conductivity ratios are only known to within an order of magnitude (Law, 1993), and may vary across the head. In addition, there is substantial variation in the thickness of each layer in both adults and children. Nevertheless, the four spheres model is a valuable simulation tool which provides reasonable estimates (often within 10-20%) of scalp potentials in comparisons with more realistic finite element models of the head (Yan et al., 1991).

2.2 Current sources in the brain

A cortical macrocolumn of diameter 3-4 mm contains approximately 10^6 neurons and 10^{10} synapses (Nunez, 1995). The polarization of this volume of tissue is the sum of microsources at the postsynaptic membranes and other remote membrane surfaces, and can be approximated as the dipole moment per unit volume. At this spatial scale, cortical tissue appears to demonstrate homogeneous statistical properties (Abeles, 1982). This is also the spatial scale considered to be at or beyond the limit of spatial resolution with scalp EEG or MEG (Cohen et al., 1990). Activity distributed throughout the entire cortex can be represented by several thousand of these dipole sources oriented perpendicular to the cortical

surface. Sources in the gyral surfaces are mostly oriented radial to the scalp surface, while sources in the sulcal walls are mostly tangential to the scalp surface.

The scalp potentials due to a radial and tangential dipole at different depths are shown in Figure 1. The dipoles were placed within the brain sphere of the four concentric spheres model of the head described in Section 2.1. The source depths are measured from 2 mm below the spherical cortical surface of 8 cm, to account for the thickness of the grey-matter. Since tangential dipoles represent sulcal walls, they are placed deeper than radial sources. In each plot, the potentials are plotted against tangential distance along the scalp surface. For the radial source, the potential distribution is spherically symmetric, with a peak directly above the source. For the tangential source the potential distribution is antisymmetric with a positive and negative (not shown) peak of equal and opposite amplitude on either side of the source. These peaks are not directly above the tangential source but rather at a distance of 2-5 cm along the scalp depending on the source depth. As sources are placed deeper, their contribution to nearby (< 5 cm) electrodes on the scalp surface is rapidly reduced. By contrast, their contribution to distant (10-30 cm) electrodes slowly increases. At a large source-electrode separation the contribution of a source to the electrode is not very sensitive to either source depth or separation distance, but will have sign dependent on orientation. Superficial sources contribute a strong potential that is restricted in extent to nearby electrodes on the scalp, and are thus the most likely sources to be accurately localized with scalp recordings.

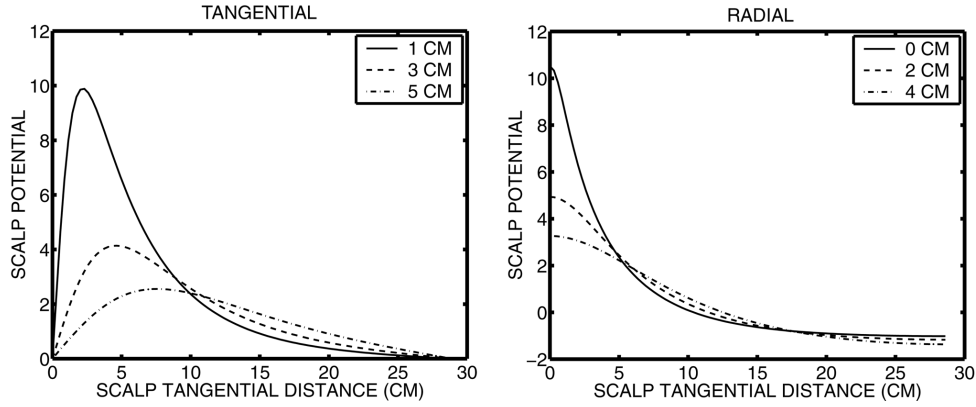


Figure 1. Scalp potentials due to a radial and a tangential dipole at different depths.

2.3 Transfer function estimates

The volume conduction properties of the head can be quantified in terms of transfer functions between the cortical source distribution and the potential distribution in the head. The scalp surface potential due to a radial dipole at an arbitrary location in spherical coordinates (r' , θ' , ϕ') is readily obtained from the four spheres model and the addition theorem for spherical harmonics $Y_{nm}(q, f)$ as the Green's function (Srinivasan et al., 1996):

$$G_{scalp}(\theta, \phi) = \sum_{n=1}^{\infty} \frac{4\pi H_n(r')}{2n+1} \sum_{m=-n}^n Y_{nm}^*(\theta', \phi') Y_{nm}(\theta, \phi) \quad (1)$$

Here, the H_n are determined by the four concentric spheres model parameters (layer thicknesses and conductivities) and the source's radial position. The spherical harmonics are the orthogonal basis set on a spherical surface, analogous to sinusoidal functions in the time domain. Examples of spherical harmonics are given in Figure 2. If the current distribution at a fixed depth (for example, sources in the superficial gyri are 2 mm below the cortical surface with $r' = 7.8$ cm) is $B(r', q, f)$ the scalp potential is obtained by multiplying the source distribution by the Green's function and integrating over the source distribution. Any radial source distribution at a fixed depth r' can be expressed as a sum over spherical

harmonics:

$$B(r', \theta', \phi') = \sum_{n=1}^{\infty} \sum_{m=-n}^n B_{nm} Y_{nm}(\theta, \phi) \quad (2)$$

Multiplying the Green's function (Eq. 1) by the source distribution (Eq. 2) and integrating over the source distribution results in the scalp potential (V):

$$V(\theta, \phi) = \sum_{n=1}^{\infty} \sum_{m=-n}^n \frac{4\pi}{2n+1} H_n B_{nm} Y_{nm}(\theta, \phi) \quad (3)$$

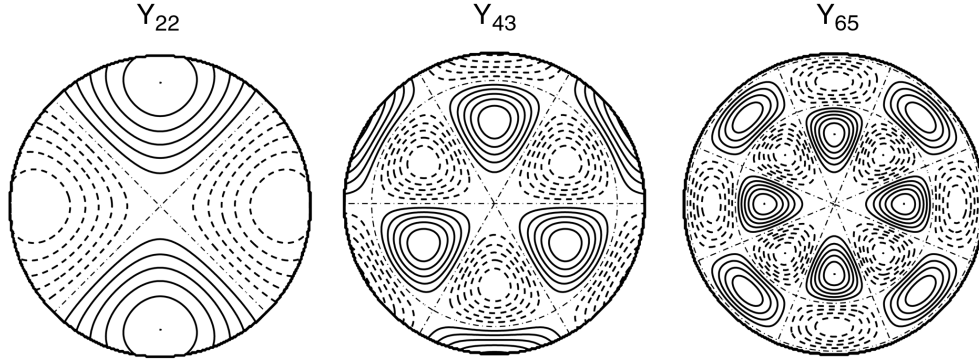


Figure 2. Topographic maps of example spherical harmonics $Y_{nm}(q,f)$. The indices n and m determine the spatial frequency in the elevation and the azimuth respectively. These topographic maps show an elevation of 0-120 degrees and an azimuth of 0-360 degrees projected onto a plane.

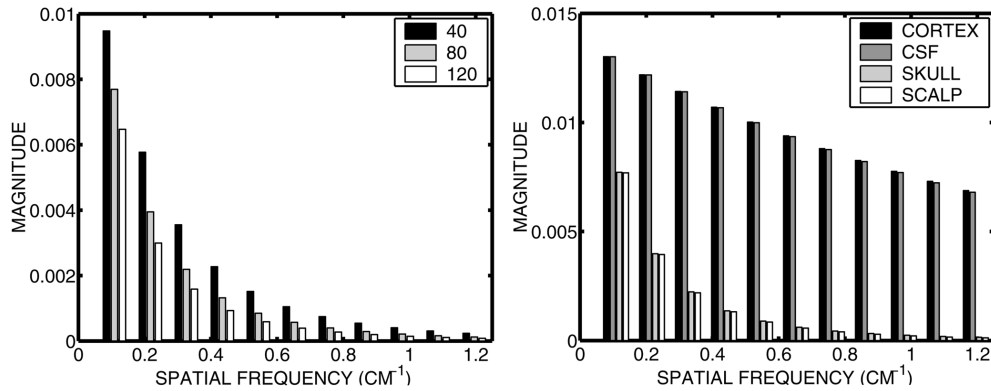


Figure 3. Transfer function between a spherical surface of radial sources (representing the gyri) and potentials in the four spheres model. Left: transfer function estimates for scalp potentials for several values of $s_{\text{brain/skull}}$. Right: transfer function estimates at the surface of each layer of the four spheres model. In this plot $s_{\text{brain/skull}}$ is fixed at 80.

Thus, the transfer function between radial cortical sources at a fixed depth (r') and scalp potentials is a only a function of spatial frequency,

$$T_{\text{scalp}}(n) = \frac{4\pi}{2n+1} H_n(r') \quad (4)$$

The magnitude of this transfer function is plotted as a function of spatial frequency in Figure 3 for different values of the $s_{\text{brain/skull}}$. The spatial frequency of a spherical harmonic of degree n is $k = (n+1)/R$, where R is the scalp radius. In all three cases, the transfer function of the head behaves like a low-pass spatial filter, preferentially transmitting to the scalp broad spatial patterns of activity over focal spatial patterns of activity. The low-pass filtering is not particularly sensitive to the conductivity ratio. As skull conductivity decreases relative to brain conductivity, amplitude is reduced at all spatial frequencies. The plot is cut-off at a spatial frequency 1.2 cm^{-1} , which is the limit of resolution with a scalp electrode spacing of 2.5 cm. There is very little power contributed by higher spatial frequencies, which suggests that this electrode spacing may be adequate to sample the scalp potentials without aliasing (Srinivasan et al., 1998b), although empirical tests with larger numbers of electrodes are needed.

Directly following Eqs. 1-3, the transfer function can be computed for the potentials at any surface in the four spheres model. The right side of Figure 3 shows the transfer function between the surface of radial dipoles at a depth of 2 mm and the potential "recorded" at the surface of the cortex, the CSF layer, the skull, and the scalp. Between the inner (CSF) and outer (skull) surfaces of the skull, there is a dramatic reduction in the magnitude of the potentials, which is more severe at higher spatial frequencies. Thus, it is the skull that acts as a low pass spatial filter on the cortical potentials. One should note as well that at the limit of spatial resolution shown here, $k = 1.2 \text{ cm}^{-1}$, cortical potentials still receive strong contributions from higher spatial frequencies. Thus, a much higher sampling density is required for direct recordings from the cortical surface. The low-pass filtering of the skull is fortuitous, as it acts as an analog low-pass spatial filter, thereby minimizing aliasing effects that can result from the discrete sampling of scalp potentials (Srinivasan et al., 1998b).

The results shown here have only considered the case of superficial radial dipoles, neglecting the contribution of superficial tangential dipoles in the sulci and/or deeper sources. This has mainly been for mathematical convenience. For tangential dipoles, orientation also plays a strong role, and is largely determined by the geometry of the folds of the cortex. Tangential dipoles are subject to cancellation effects, since each sulcal wall faces an adjoining wall. If both walls are active and synchronous, they form two opposing current sources that will mostly cancel each other out. However, the general idea of low-pass spatial filtering also applies to tangential dipoles. The spatial frequency dependent parameters H_n in Eqs. 1 and 3 are identical for radial and tangential dipoles, and the cortical surface potential due to tangential dipoles will still be low-pass filtered by the skull. Deeper sources are more severely low-pass spatially filtered by the skull, as evidenced by the even spatial distribution of the potentials shown in Figure 1. Thus, the potentials at high spatial frequencies are only due to superficial sources. The high spatial frequencies contribute much of the potentials at short ($< 5 \text{ cm}$) tangential separation between source and electrodes.

3. Surface Laplacian estimates

The surface Laplacian method is a direct approach to improve the spatial resolution of each EEG electrode. The surface Laplacian is the second spatial derivative of the scalp potentials along an approximation to the scalp surface, which provides estimates of the cortical surface potentials from the scalp potentials. The physical basis of surface Laplacian estimation will be reviewed and estimates of the spatial resolution of the Laplacian will be presented. A 3-dimensional spline algorithm is introduced for Laplacian estimation. This algorithm allows for control of the amount of spatial smoothing based on physical properties of the EEG electrode montage. This spline can be used to obtain surface Laplacians along a realistically shaped scalp surface.

2.1 Physical basis of the surface Laplacian

The transfer functions shown in Figure 3 suggest some intuitive ideas about EEG recordings on the cortex and the scalp. First, simply increasing the number of electrodes will not

improve the spatial resolution of EEG because of the severe low-pass filtering of the skull. The cortical surface potential receives a much larger contribution from higher spatial frequencies. Because the skull is such a poor conductor, current flow in the skull will be largely radial, flowing from the inner to the outer surface of the skull. Based on Ohm's Law and current conservation the following relationship has been derived (Katznelson, 1981):

$$V_{CSF} = V_{skull} + \frac{\rho_{skull}}{\rho_{scalp}} d_{skull} d_{scalp} L_{scalp} \quad (5)$$

Here V_{CSF} and V_{skull} are the potentials at the inner and outer surfaces of the skull, r_{skull} and r_{scalp} are the resistivities of the skull and the scalp, d_{skull} and d_{scalp} are the thicknesses of the skull and scalp, and the surface Laplacian $L_{scalp} = \nabla^2 V_{scalp}$. From Figure 3 we observe that $V_{CSF} \sim V_{cortex}$ and that $V_{skull} \ll V_{CSF}$, so that in Eq. 5, $L_{scalp} \approx V_{cortex}$. Thus, the surface Laplacian of the scalp potentials can be used to estimate the cortical surface potentials. Good estimates of the values of the tissue conductivities are not needed to use the surface Laplacian to estimate the cortical surface potential, but the approximation in Eq. 5 is valid only that the skull is a much poorer conductor than the other layers.

Figure 4 shows the fall-off with tangential distance for a radial and a tangential dipole for the cortical surface potential and the surface Laplacian. By comparison to the fall-off for scalp potentials, both the cortical surface potential and the surface Laplacian contribute minimal signal to distant electrodes. Furthermore, the contribution of deeper sources is very limited. Both cortical surface potentials and the surface Laplacian appear to be good estimates of local superficial cortical sources, with minimal contributions from either distant or deep sources. This observation is consistent with lead-field analysis of Laplacian electrodes, which have also demonstrated their high spatial resolution (Malmivuo and Plonsey, 1995).

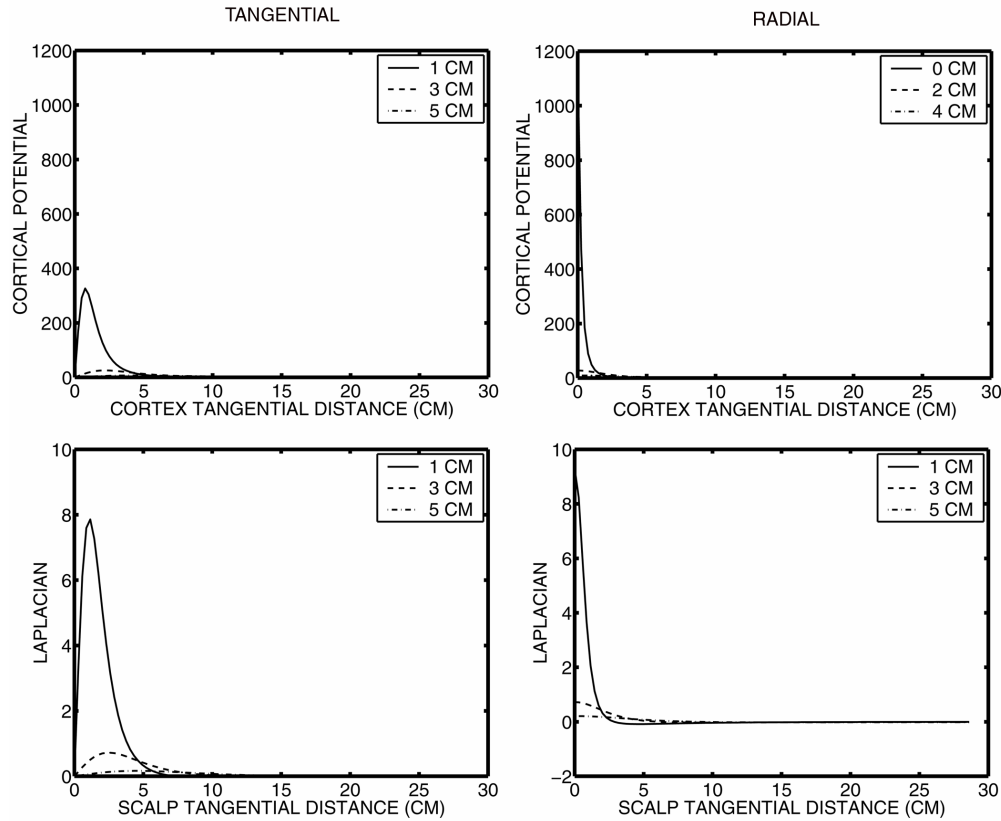


Figure 4. Cortical surface potentials and scalp surface Laplacians due to a tangential and radial dipole source.

3.2 Transfer function estimates

Transfer function estimates for a spherical surface of superficial ($r = 7.8$ cm) radial dipole sources for the surface Laplacian and the cortical surface potential as shown in Figure 5. The transfer function for the cortical surface potential falls off slowly with spatial frequency, and is independent of $s_{\text{brain/skull}}$. The surface Laplacian shows similar behaviour to the cortical surface potentials at high spatial frequencies. However, the Laplacian is sensitive to $s_{\text{brain/skull}}$, which can have a large impact on overall magnitude. Since the spatial sampling of EEG restricts the highest spatial frequencies observed, Laplacian estimation methods must apply a measure of smoothing to roll-off the higher spatial frequencies beyond the spatial Nyquist, which is usually $k \sim 1\text{cm}^{-1}$ for high density EEG montages (64-128 electrodes). When comparing the Laplacian EEG in two states an individual, this will not influence results. When comparing across groups, e.g. children of different ages, the influence of skull conductivity differences between the groups on the Laplacian estimates must be considered.

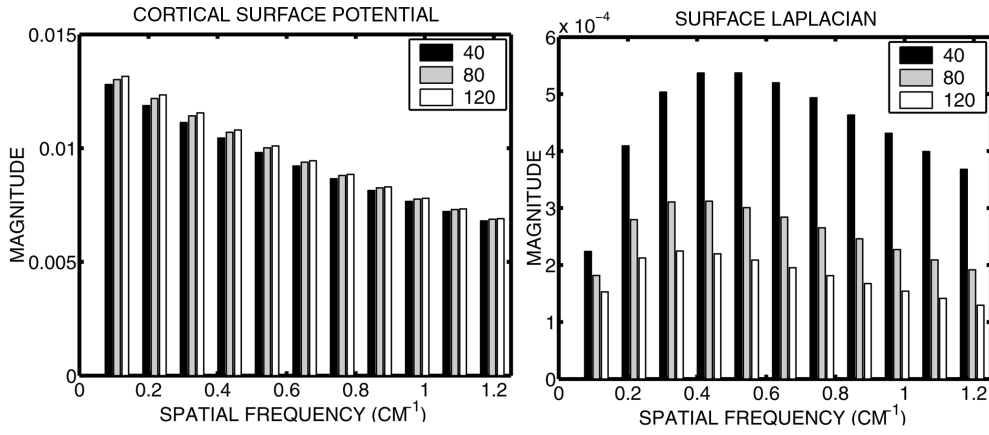


Figure 5. Transfer function estimates for cortical surface potentials and scalp surface Laplacians. Left: transfer function estimates for cortical surface potentials for several values of $s_{\text{brain/skull}}$. Right: transfer function estimates for surface Laplacians for several values of $s_{\text{brain/skull}}$.

3.3 The 3-dimensional spline-Laplacian

A three-dimensional spline interpolant function from n samples in three dimensional space can be defined as (Perrin et al., 1987; Law et al., 1993):

$$V(x, y, z) = Q(x, y, z) + \sum_{i=1}^n p_i K(x - x_i, y - y_i, z - z_i)$$

$$Q(x, y, z) = q_1 + q_2 x + q_3 y + q_4 x^2 + q_5 xy + q_6 y^2 + q_7 z + q_8 zx + q_9 zy + q_{10} z^2 \quad (6)$$

$$K(x, y, z) = (x^2 + y^2 + z^2)^2 \log(x^2 + y^2 + z^2 + w^2)$$

The coefficients p and q depend on the data, and are calculated by solving a matrix equation (Law et al., 1993). To contrast this spline to spherical splines (Perrin et al., 1989), the 3-dimensional spline has been rewritten as a spherical harmonic expansion (Srinivasan et al., 1996). This expansion was used to demonstrate that the logarithmic basis function used by this 3-dimensional spline is an infinite-order spherical harmonic expansion which intrinsically smooths the data at high spatial frequencies to prevent spatial aliasing. The amount of smoothing is controlled by the parameter w , which theoretically should be set to the electrode diameter (including gel or saline) in order to distribute the loading of the interpolant function by the data over a finite sized area rather than a point. However, in cases where the data has been spatially undersampled (< 64 electrodes), the electrodes should be

enlarged to minimize erroneous estimates of undersampled higher spatial frequencies. This can be effected by setting w to interelectrode distance minus the electrode diameter.

The Laplacian is calculated from the same coefficients p , and q , by applying them to the Laplacian of the interpolant function, Eq. 6. This has been carried out for spherical and ellipsoidal approximations to the head surface showing comparable results (Law et al., 1993). The three-dimensional spline also offers an important advantage of surface independence. By using the 3-dimensional spline function, the potential can be interpolated along a realistic scalp surface, if both electrode positions and the scalp surface position are accurately known. If the scalp surface normals $\mathbf{n}(x,y,z) = (n_x, n_y, n_z)$ are also known the Laplacian can be taken along the realistic scalp surface as:

$$\nabla_{surf}^2 = \left(1 - n_x^2\right) \frac{\partial^2}{\partial x^2} + \left(1 - n_y^2\right) \frac{\partial^2}{\partial y^2} + \left(1 - n_z^2\right) \frac{\partial^2}{\partial z^2} - n_x n_y \frac{\partial^2}{\partial x \partial y} - n_x n_z \frac{\partial^2}{\partial x \partial z} - n_y n_z \frac{\partial^2}{\partial y \partial z} \quad (7)$$

As discussed by Babiloni (Babiloni et al., 1996), there can be improvements in the accuracy of Laplacian estimates by extracting the scalp surface from an MRI to use for derivative estimates. However, as comparisons between spherical and ellipsoidal Laplacians have shown (Law et al., 1993), even on a spherical surface, the Laplacian is a robust estimator of cortical surface potentials.

4. An example simulation

Several thousand simulations of complex source configurations have been carried out to verify the accuracy of the three-dimensional spline Laplacian, and to validate the Laplacian as an estimate of cortical potential. An example of a complex source distribution consisting of a spherical surface of radial dipole sources 2 mm below the surface of the brain spheres in the four concentric spheres model of the head is shown in the upper left panel of Figure 6. In this plot the black dots represent negative sources while the white dots represent positive sources. The sources are of variable magnitude, which is not shown by the figure. Note that there are three major "clumps" of source activity. In the top left

of the distribution, there is a black square representing strong negative sources that are at ten times the magnitude of the background activity. There are two major white clumps, at the center and lower right, which are positive sources at twice the magnitude of the background activity. The surface area of the central clump is four times that of the peripheral clumps. The upper right panel of Figure 6 shows the scalp potentials due to the cortical source distribution in the upper left panel. The negative clump and large positive clump both generate scalp potentials of comparable magnitude. Indeed, if armed with only this topographic map, one could readily erroneously fit this distribution by a deep tangential dipole with a large magnitude.

The lower left and right panels of Figure 6 shows the cortical surface potential and scalp surface Laplacian generated by the same distribution. The Laplacian estimate is a remarkably accurate reflection of the major "clumps" of source activity on the brain surface, correctly identifying both their relative magnitude and their location. It is interesting to note that the cortical potentials are relatively blind to the large central clump. This feature makes a comparable contribution to the scalp potential as the high magnitude negative source. This reflects that fact that the scalp potentials are low-pass filtered, averaging together broad areas of the cortical surface. When multiplied by the surface area, it is evident that the small-surface-area high-magnitude negative clump contributes the same energy as the large-surface-area low-magnitude positive clump. Both the Laplacian and the cortical surface

potential is a measure of the strength of local sources and is relatively insensitive to the surface area of a distribution of activity.

5. Discussion

Simulations and theoretical arguments have been presented here to support the contention that the scalp surface Laplacian is a reasonable estimate of cortical surface potentials. Further theoretical analyses of the Laplacian method have been carried out to demonstrate that the Laplacian removes the effects of volume conduction on EEG coherence, allowing each electrode to be a relatively independent measure of the superficial cortical sources within a few centimeters of the electrode (Srinivasan et al., 1998a). However, since the Laplacian is insensitive to very broad spatial patterns of activity, the Laplacian does not replace the potential data, but is a useful tool to examine aspects of the data that are unambiguously related to focal superficial sources. Experimental studies support this view that the potentials and the Laplacians provide complementary views of neocortical dynamics at distinct, but partly overlapping spatial scales (Srinivasan et al., 1999).

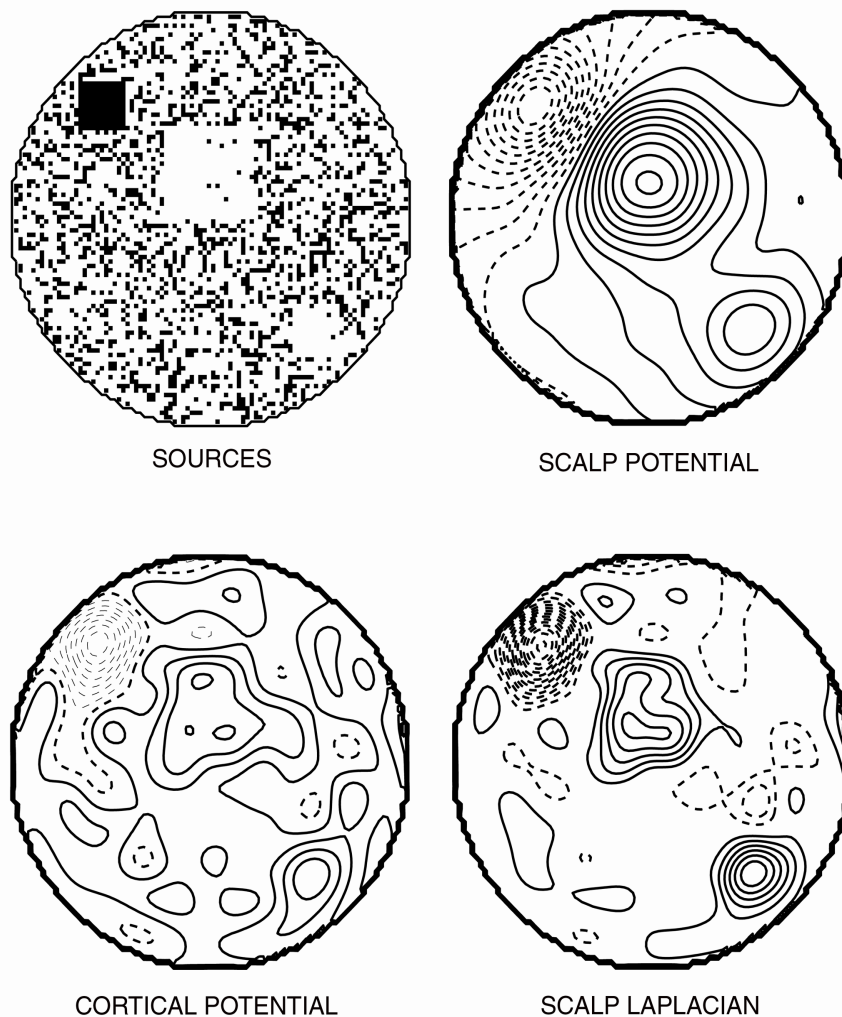


Figure 6. Example of a complex source distribution. Upper left: Sources. Black dots represent negative sources, while spaces represent positive sources. Upper Right: Scalp potential. Lower Left: Cortical surface potential. Lower Right: Scalp Laplacian. The scalp Laplacian was calculated from 111 electrodes distributed evenly across the scalp potentials (2.7 cm separation), using the 3-dimensional spline-Laplacian algorithm.

References

- [1] Abeles M: Local Cortical Circuits. Springer-Verlag, New York, 1982.
- [2] Babiloni F, Babiloni C, Carducci F, Fattorini L, Onorati P, Urbano A: Spline Laplacian estimate of EEG potentials over a realistic magnetoc-resonance reconstructed scalp surface model, *Electroencephalography and Clinical Neurophysiology*, 98:363-373, 1996.
- [3] Cohen D, Cuffin BN, Yunokuchi K, Maniewski R, Purcell C, Cosgrove GR, Ives J, Kennedy J: MEG versus EEG localization using implanted sources in the human brain, *Ann. Neurol.*, 28:811-817, 1990.
- [4] Katznelson RD: Normal modes of the brain: neuroanatomical basis and a physiological theoretical model, in Nunez PL, *Electric Fields of the Brain: The Neurophysics of EEG*, New York, Oxford, 1981.
- [5] Law SK, Nunez PL, Wijesinghe, RS: High resolution EEG using spline generated surface Laplacians on spherical and ellipsoidal surfaces, *IEEE Transactions on Biomedical Engineering*, 40:145-153, 1993.
- [6] Law SK: Thickness and resistivity variations over the upper surface of the human skull, *Brain Topography*, 6(2), 1993.
- [7] Malmivuo J, Plonsey R: *Bioelectromagnetics - Principles and Application of Bioelectric and Biomagnetic Fields*, Oxford University Press, New York, 1995.
- [8] Nunez PL, Silberstein RB, Cadusch PJ, Wijesinghe RS, Westdorp AF, Srinivasan R: A theoretical and experimental study of high resolution EEG based on surface Laplacians and cortical imaging, *Electroencephalography and Clinical Neurophysiology*, 90:40-57, 1994.
- [9] Nunez PL: *Electric Fields of the Brain: The Neurophysics of EEG*, Oxford University Press, New York, 1981.
- [10] Nunez PL: *Neocortical Dynamics and Human EEG Rhythms*, Oxford University Press, New York, 1995.
- [11] Perrin F, Bertrand O, Pernier J: Scalp current density mapping: value and estimation from potential data, *IEEE Transactions on Biomedical Engineering*, 34:283-289, 1987.
- [12] Perrin F, Pernier J, Bertrand O, Echaliier JF: Spherical splines for scalp potential and current density mapping, *Electroencephalography and Clinical Neurophysiology*, 72:184-187, 1989.
- [13] Sidman RD: A method for simulating intracerebral potential fields: the cortical imaging method, *Journal of Clinical Neurophysiology*, 8:432-441, 1991.
- [14] Srinivasan R, Murias M, Tucker DM: Estimates of the spatial Nyquist of EEG, *Behavior Research Methods, Instruments, and Computers*, 30:8-19, 1998b.
- [15] Srinivasan R, Nunez PL, Silberstein RB: Spatial filtering and neocortical dynamics: estimates of EEG coherence, *IEEE transactions on Biomedical Engineering*, 45:814-826, 1998a.
- [16] Srinivasan R, Nunez PL, Tucker DM, Silberstein RB, Cadusch PJ: Spatial sampling and filtering of EEG with spline Laplacians to estimate cortical potentials, *Brain Topography*, 8:355-366, 1996.
- [17] Srinivasan R: Spatial structure of the human alpha rhythm: global correlation in adults and local correlation in children, *Clinical Neurophysiology*, in press, 1999.
- [18] Towle VL, Syed I, Grzesczczuk R, Milton J, Erickson RK, Cogen P, Berkson E, Spire JP: Identification of sensory/motor area and pathological regions using EcoG coherence, *Electroencephalography and Clinical Neurophysiology*, 106:30-39, 1998.
- [19] Yan Y, Nunez PL, Hart RT: A finite element model of the head: scalp potentials due to dipole sources, *Medical and Biological Engineering and Computing*, 29:475-481, 1991.

